ICSV 21
13-17 July, 2014, Beijing/China

The 21st International Congress on Sound and Vibration

13-17 July, 2014, Beijing/China

EXPERIMENTAL AND NUMERICAL INVESTIGATION OF TIP CLEARANCE NOISE OF AN AXIAL FAN USING A LATTICE BOLTZMANN METHOD

Tao Zhu*, Michael Sturm and Thomas H. Carolus

Institute of Fluid- and Thermodynamic, University of Siegen, Siegen, Germany
**e-mail: tao.zhu@uni-siegen.de*

Barbara Neuhierl

Exa GmbH, Munich, Germany

Franck Pérot

Exa Corporation, Brsbane, CA, USA

The secondary flow through the tip clearance is one of the well-known sources contributing to the overall noise of axial fans. Aerodynamic losses and sound radiation increase significantly as the tip clearance is increased. The objective of this study is to revisit the mechanisms for tip clearance noise from a rotating fan impeller.
The unsteady and compressible numerical Lattice-Boltzmann-Method (LBM) is utilized which allows a direct and simultaneous prediction of both aerodynamic and acoustic field. Overall aerodynamic and acoustic fan performance data as predicted with the LBM were validated with experimental data. The agreement was quite satisfactory which justified looking at the LBM-predicted field data in detail. The flow and acoustic field in the vicinity of an axial fan impeller's tip gap revealed important details of the sound generating mechanism. A large tip clearance is responsible for a complex vortex system with a considerable degree of inherent unsteadiness. The consequences are fluctuations of static pressure in the flow field in the adjacent tip region and on the blade surfaces, more pronounced on the pressure than on the suction side. Those pressure fluctuations generate sound that is then radiated away from the complete impeller upstream into the free field with the typical hemispherical directivity pattern.

1. Introduction

The aerodynamic and aeroacoustic performance of axial fans are strongly affected by the unavoidable tip clearance. Aerodynamic losses and sound radiation increase significantly as the tip clearance is increased. Tip clearance studies have a long history. Longhouse[1] reported increased broadband noise level as result of an enlarged tip clearance. He focused on the interaction of the tip vortex with the blade tip region, but without a quantitative flow analysis. You et al.[2] illustrated the complex tip vortex structures as obtained from a Large Eddy Simulation (LES) of a blade cascade with moving wall in a stationary system, including the dominant tip leakage vortex (TLV), the tip separation vortex (TSV) and other induced small scale vortices. The effect of the size of the tip clearance on generation and evolution of vortices was also discussed by You et al.[3]. Fukano and Jang[4] analyzed the tip clearance flow utilizing two hot-wire probes in the rotating blade passage. They proved that the noise due to tip clearance flow was linked to velocity fluctuations in the blade passage. A detailed aeroacoustic investigation of an isolated stationary airfoil placed adjacent to a wall with a well defined gap was carried out by Grilliat et al.[5] and Jacob et al.[6]. They measured

pressure fluctuations on the airfoil surface, flow velocities and the flow induced near and far field acoustics. Eventually they identified two mechanisms of tip leakage broadband self noise. A detail experimental study on a low Mach number axial fan was carried out by Kameier and Neise[7] and März et al.[8]: Large tip clearances and high blade loading caused a narrow-band spectral hump in the noise signature which was attributed to rotating flow instability in the gap region. Neuhaus and Neise[9] tried to control tip clearance noise by active flow control, and, more recently, Corsini et al.[10] and Aktürk and Camci[11, 12] by passive devices such as tip end-plates and squealers.

The objective of this study is to revisit the mechanisms for tip clearance noise from a rotating fan impeller. Aerodynamic and acoustic measurements are compared with numerical results from an unsteady compressible numerical Lattice Boltzmann method (LBM). As compared to the more classical approach where unsteady flow field data from an unsteady Reynolds averaged Navier-Stokes and/or large eddy simulation are fed into an acoustic Ffowcs Williams and Hawkings (FWH) analogy (see e.g. Zhu and Carolus[13]), the LBM promises a direct and simultaneous prediction of acoustic field data. It is of interest, how LBM-data compare to experimental results and how the LBM-method may foster the understanding of tip clearance noise.

2. Fans investigated and test rig

2.1 Impellers investigated

An axial fan impeller, Figure 1 (left), was designed with an in-house blade element momentum based design code for low pressure axial fans (dAX-LP, see Carolus[14]). Differently from a free vortex design the design blade loading is 70% at hub and 120% at tip, distributed approx. linearly in spanwise direction. The loading of the blade tip is done intentionally to provoke strong secondary tip flow that is eventually responsible for tip clearance noise. Further design parameters are compiled in Table 1. Two impellers with different diameters were manufactured, providing a variation of tip clearance; one with a large tip clearance ratio s/D_a = 1.0% (i.e. a clearance of 3 mm) and one with an extremely small gap of s/D_a = 0.1% (i.e. a clearance of 0.3 mm). To ensure a very homogenous inflow an AMCA standardized nozzle with elliptical contour was employed on the test fan unit. Thin supporting struts were mounted one duct diameter downstream of the rotor, so that rotor/strut interaction was minimized, Figure 1 (right).

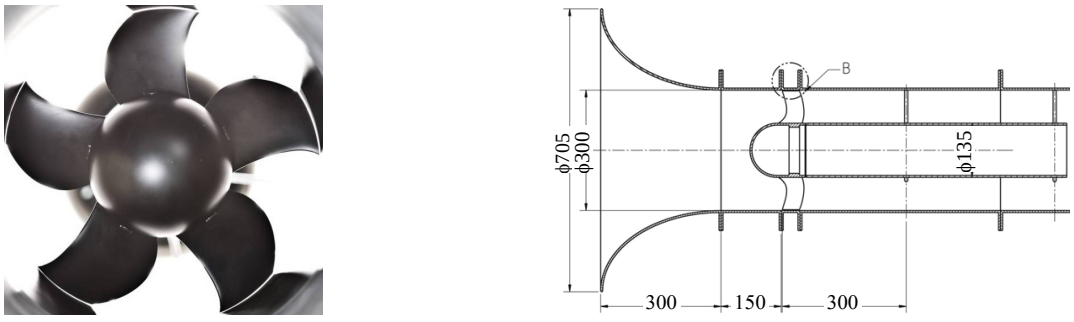

Figure 1. Manufactured impeller and fan assembly.

Table 1. Important impeller design parameters.

Duct diameter	D_a	[mm]	300	Design flow rate	$\dot{V}$	m^3/s	0.650
Hub to duct ratio	ν	[-]	0.45	Density of air	ρ	kg/m^3	1.2
Number of blades	z	[-]	5	Rotational speed	n	rev/min	3000

2.2 Aerodynamic and acoustic measurements and data evaluation

The aerodynamic fan performance was determined on a standard plenum test rig for fans according to the German standard DIN 24163. The aeroacoustic investigations were carried out on a standardized acoustic duct test rig for fans with a semi-anechoic room (4.50 m×3.50 m×3.23 m) according to DIN ISO 5136, Figure 2. The impeller takes the air from a large semi-anechoic room

and exhausts into a duct with an anechoic termination. The flow rate is controlled by a throttle downstream of the termination and is determined by a calibrated hot film probe in the duct.

The suction side sound pressure level L_{p5} is measured in the free field of the anechoic room by three microphones (Brüel & Kjaer, type 4190), placed on a hemispherical measurement surface around the inlet. All time signals were captured with a sampling frequency $f_{s\text{-}Exp}$ = 25.6 kHz. The spectral analysis is based on the power spectral density level (PSDL) which was obtained by the function *pwelch* in MATLAB® Vers. 7.11. The parameters chosen for *pwelch* were *window* = *hann(nfft)*, *noverlap* = 0, *nfft* = *length(time signal)/T*. The spectra from the windows have been averaged according to the measurement time T in second, their final frequency resolution is Δf_{Exp} = 1 Hz. For all levels, the reference pressure is $p_0 = 2 \cdot 10^{-5}$ Pa. All overall levels are the sum of narrow band levels from 100 Hz to 10 kHz.

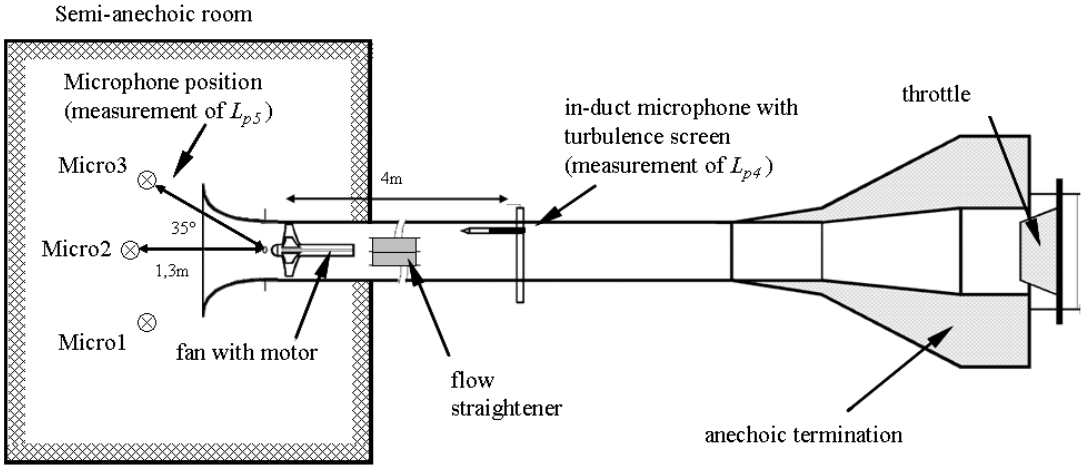

Figure 2. Standard acoustic duct test rig with semi-anechoic room (not to scale)

3. Numerical Approach

3.1 Lattice-Boltzmann-Method

To predict the unsteady flow phenomena associated with the tip flow and the generation and radiation of sound, a Lattice-Boltzmann-Method (LBM) is utilized. LBM-based methods are by nature explicit, transient and compressible. Unlike conventional CFD methods based on discretizing the macroscopic continuum equations, LBM starts from "mesoscopic" kinetic equations, i.e. the Boltzmann equation, to predict macroscopic fluid dynamics[15, 16]. The basic idea of LBM is to track the advection and collisions of fluid particles. Since the average number of particles in a representative volume of fluid far exceeds the compute power required to track them individually, the particles are grouped into a set of discrete *i*-directions. The computation follows the particle distribution function f_i which represents the number of particles in a unit of volume at a specific time and location moving with velocity c_i. As in statistical physics, the flow variables such as density and velocity are determined by taking the appropriate moments, i.e. summations over the set of discrete directions, of the particle distribution function.

In this study the commercial code PowerFlow™ in the version 4.4d is used. In order to model the effects of unresolved small scale turbulent fluctuations, in this code the Lattice-Boltzmann equation is extended by replacing its molecular relaxation time scale with an effective turbulent relaxation time scale derived from a systematic Renormalization Group (RG) procedure, see details in Chen et al. [17-19]. A turbulent wall-model, including the effect of pressure gradients, is also integrated into the solver. This method is called Very Large Eddy Simulation (VLES) and has been validated and used for several aeroacoustic problems[20-22]. The LBM scheme is solved on a grid composed of cubic volumetric elements, so called voxels, using a Variable Resolution (VR) strategy, where the grid size changes by a factor of two for adjacent resolution regions. For the simulations of flows in domains consisting of rotating and stationary regions, the computational domain is divided into a so called "body-fixed" Local Reference Frame (LRF) and a "ground-fixed" reference frame domain, connected by an interface, see details in Zhang et al.[23].

3.2 Numerical setup

The computational domain is the complete acoustic test rig from Figure 2 in full scale. For simplicity all inner walls of the semi-anechoic room (i.e. even the floor) are defined as porous. Both, air inlet and outlet region, are modeled as damping zones to avoid acoustic reflections. All other surfaces (nozzle, duct, fan impeller and fan hub) are specified as rigid walls. The mass flow according to the required fan operating point is specified at the inlet. Free exhaust at ambient atmospheric pressure is assumed at the outlet. The simulation is restricted to the fan design point, i.e. a flow rate 0.65 m^3/s. A LRF-domain around the rotating fan impeller is discretized using the finest grid resolution of Δx = 0.5 mm (VR10) corresponding to 600 voxels across the duct diameter. The VR-zones are denoted in Figure 3. The regions around the "microphone probes" are resolved spatially with Δx_{mic} = 8.0 mm (VR6). The large tip clearance is resolved with 6 voxels, the small tip clearance is replaced by s/D_a = 0.0%, i.e. tip clearance is completely neglected.

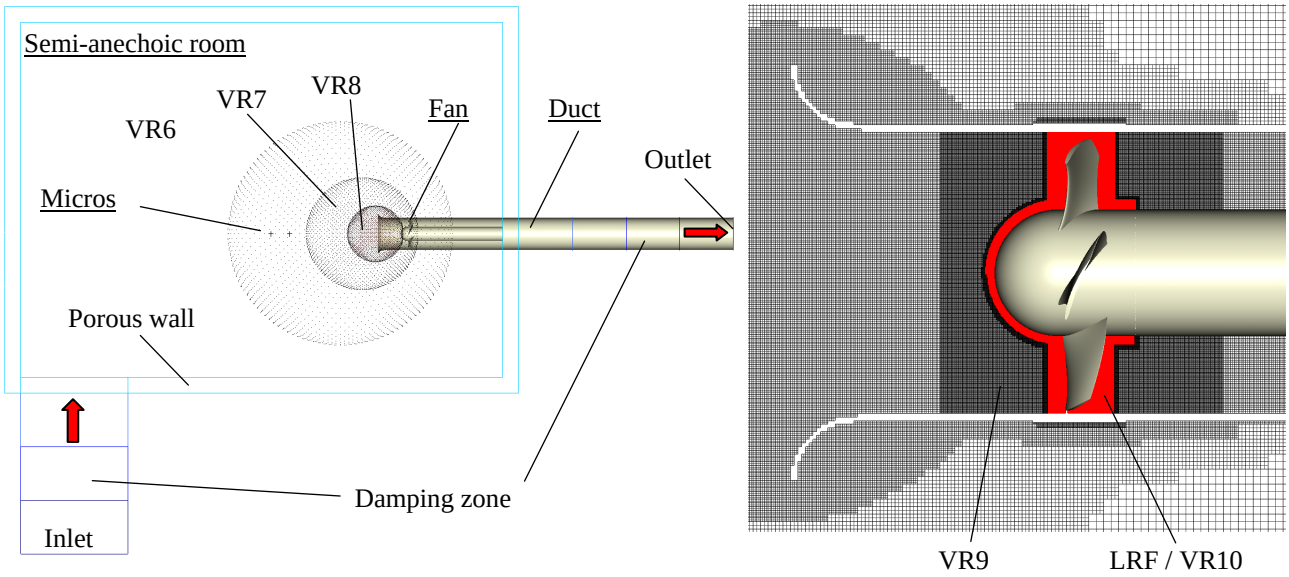

Figure 3. Simulation-domain including the semi-anechoic room and test rig duct (left), mesh detail in the fan section with LRF-domain (right, red).

The calculation is performed over an overall time interval $T_{sim} \approx 1$ s corresponding to appr. 50 impeller revolutions upon arriving at the statistically stable fan operating (= design) point. The simulation time step is $\Delta t = 8.2 \cdot 10^{-7}$ s in VR10. The data at the monitoring points in the acoustic far field, i.e. at the microphone probe positions, are captured with a sampling frequency $f_{s\text{-}Probe.}$ = 75822 Hz, the hydrostatic pressure fluctuations on the blade surface and in an adjacent annular volume with $f_{s\text{-}SurVol.}$ = 18955 Hz. All spectra are evaluated from the raw LBM data using the same method described in section 2.2 but with a frequency resolution of Δf_{LBM} = 5 Hz.

The fan's overall pressure rise is evaluated in planes appr. one duct diameter up- and down stream from the fan impeller, area-averaged in each plane and time-averaged during ten revolutions.

4. Results

4.1 Measured and LBM-predicted aerodynamic and acoustic overall characteristics

The aerodynamic overall performance characteristics in terms of Δp_{ts}, η_{ts} as a function of $\dot{V}$ are shown in Figure 4 (left). The effect of the tip clearance on the aerodynamic characteristics is rather obvious: Pressure rise and efficiency drop and the onset of stall moves to higher flow rates as the tip clearance is increased. The LBM-prediction at design operation point is rather satisfactory.

The acoustic performance characteristics in terms of overall sound pressure level at Micro-2 $L_{p\text{-}Mic2}$ as a function of $\dot{V}$ are shown in Figure 4 (right). With the small tip clearance the sound pressure level is nearly constant in the "healthy" flow regime down to the anticipated dramatic jump upon onset of stall, whereas for the large tip clearance the sound pressure level increases monotoni-

cally as the flow rate is decreased. The sound pressure as predicted from LBM reflects the effect of the tip clearance quite well: Although the absolute values are somewhat under predicted, LBM and experiments show about 10 dB increase due to the large clearance. The prediction of overall characteristics might be improved employing a finer grid resolution in the further work.

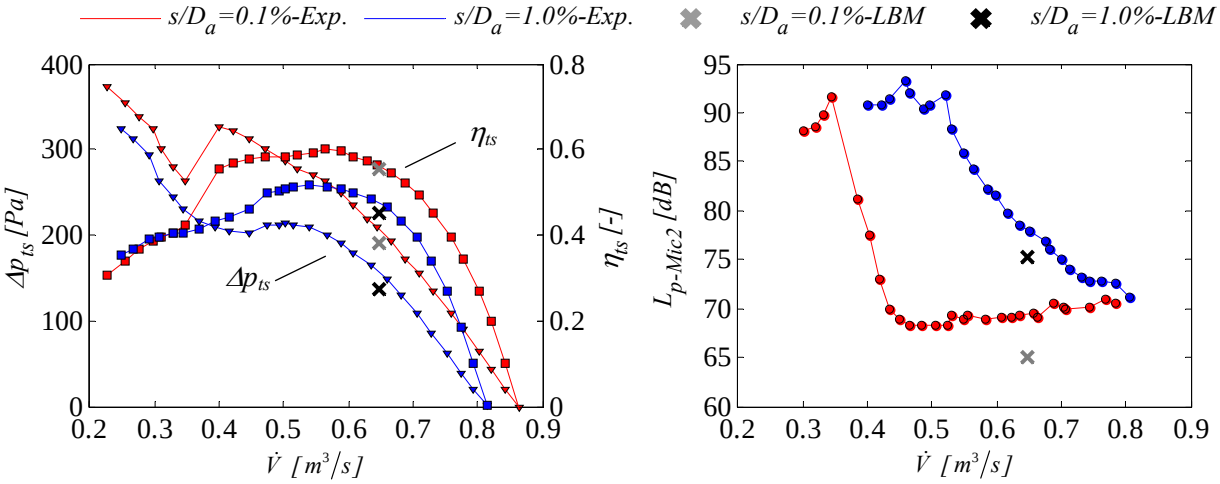

Figure 4. Aerodynamic characteristic (left) and acoustic (right) characteristics.

The sound pressure spectra at a position corresponding to Micro-2 are depicted in Figure 5, when the impellers are operated at their design point. Both, measurements and LBM-prediction, show that the broadband sound is enhanced by increasing the tip clearance. Looking at the broad band components the agreement between experimentally determined and predicted spectra is relatively satisfactory. The peaks at blade passing frequency (BPF) and its first harmonic (250 and 500 Hz, respectively) are not captured by the LBM simulation. However, according to recent experimental investigations of the same fan/test rig assembly by Sturm and Carolus[24], BPF sound from this isolated axial fan is related to large scale inflow distortions caused by the slow flow in the room the fan takes its air from. Given the short physical simulation time of approximately one second it is clear that this slow flow in the room has not developed yet. The peaks at 380 and 760 Hz predicted by the LBM for the case of a large tip clearance may be attributed to some kind of rotating instability, becoming dominant at part load operation of the fan as shown by Zhu and Carolus[13]. The raising of the spectra up approx. 6 kHz should be improved using a finer space resolution at microphone position.

4.2 LBM-predicted flow and acoustic field

It is an inherent advantage of any numerical field method that all overall quantities are derived from basic flow or acoustic field variables. Here, the satisfactory agreement of the LBM-predicted overall results encourages to analyzing the LBM-predicted flow field in more detail. In the following paragraphs we will focus on unsteady phenomena in a frequency band between 1 and 2 kHz only. All flow patterns are constructed from band pass filtered data between 1 and 2 kHz. For that the filtered signals are transformed back to the time domain employing a reverse Fast Fourier Transform.

A detailed insight of how the hydrodynamic and acoustic fields are linked becomes obvious from Figure 6. We will have a closer look at the blade surface in tip region and an annular region in the free field around the blade tips containing the upper half of the blades. Applying the λ_2-criterion on the instantaneous velocity field at a certain time step one obtains the grey colored filaments indicating vortex structures of various scales in the flow field (left and middle column in Figure 10). The red and blue isosurfaces in the free field visualize the pattern of instantaneous pressure. As expected, without tip clearance the vortex structure only stems from the flow separation at the trailing edge. The large tip clearance, however, is responsible for a distinct system of vortices originating right from the leading edge in the gap. It causes strong pressure fluctuations on the blade surface in the tip region (Figure 6, right column, lower row).

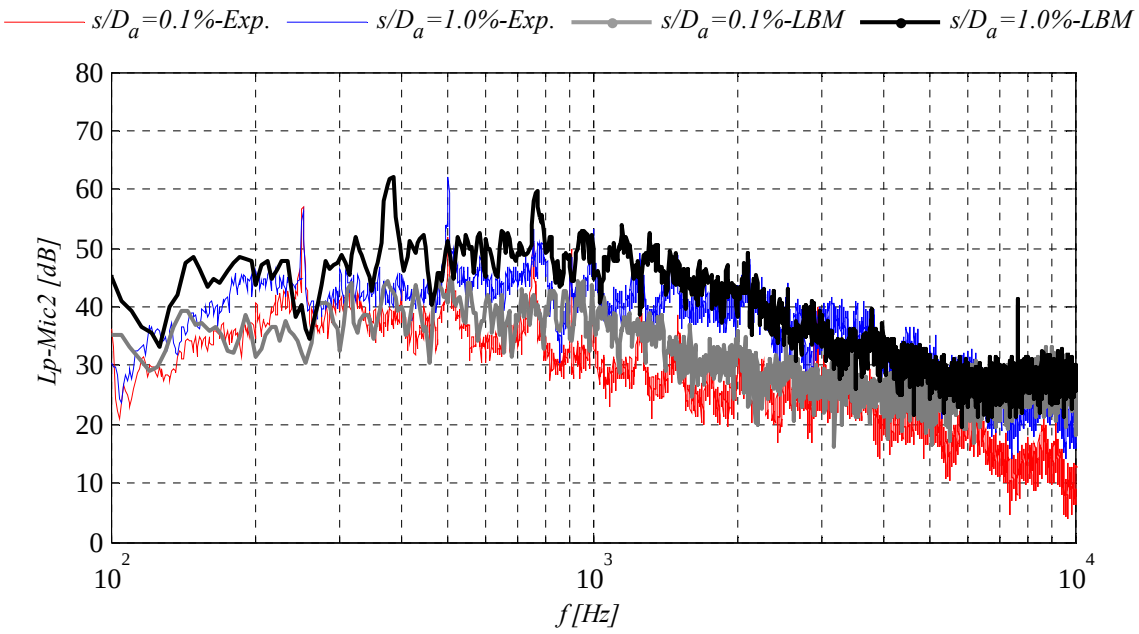

Figure 5. Micro-2 sound pressure spectra at design point (Δf_{Exp} = 1 Hz, Δf_{LBM} = 5 Hz).

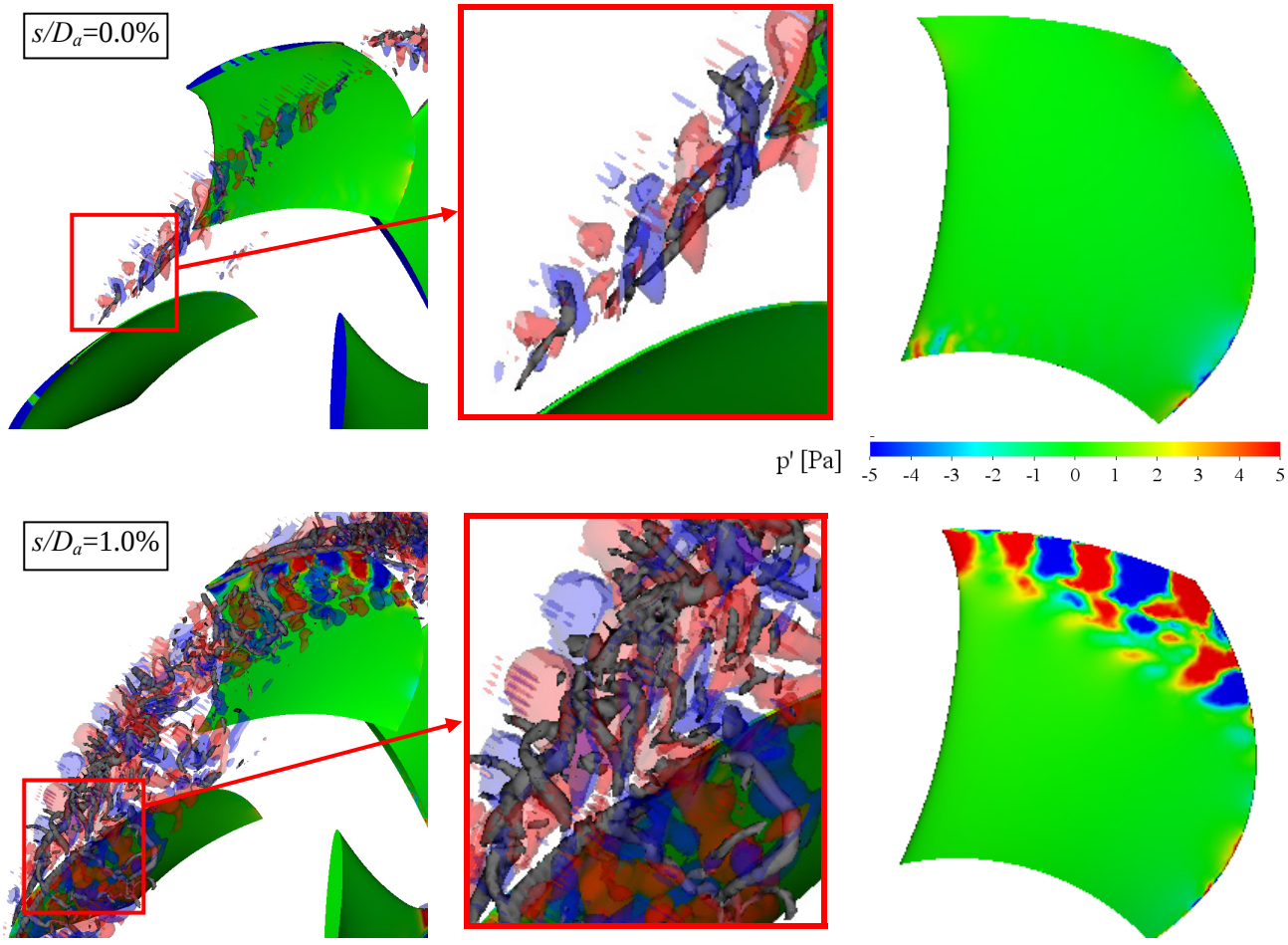

Figure 6. Left and middle column: Instantaneous vortex filaments (grey isosurface of λ_2 with value of -800) and instantaneous isosurfaces of pressure in the flow field (blue: < -5 Pa, red: > +5 Pa); right column: Instantaneous surface pressure on blade pressure side (blue: < -5 Pa, red : > +5 Pa); data band pass filtered (1 to 2 kHz).

As a summary Figure 7 shows the areas of the blade surfaces that are contaminated by excessive pressure fluctuations (in terms of power spectral density level during 10 revolutions). The

small area of contamination in the hub region close to the trailing edge is independent of the tip gap. This confirms that sound in the frequency band 1 to 2 kHz is indeed linked to vortex induced surface pressure fluctuations in the blade tip region. Clearly the tip vortex system affects the pressure side by far more than the suction side.

The resulting field of instantaneous acoustic pressure far upstream of the impeller is depicted in Figure 8. As before we confine ourselves to fluctuations in the frequency band 1 to 2 kHz. It is worth to mention that exclusively the pressure in the stationary frame is visualized, not in the LRF-domain. Without tip clearance the monitoring points Micro 1 to 3 only see quite weak waves, whereas with the large tip clearance much stronger acoustic pressure fluctuation arrive at these monitoring points. This is in line with the sound pressure spectra from Figure 5. A time series of such instantaneous pictures could be used to visualize sound waves propagating from the impeller through the nozzle to the far field.

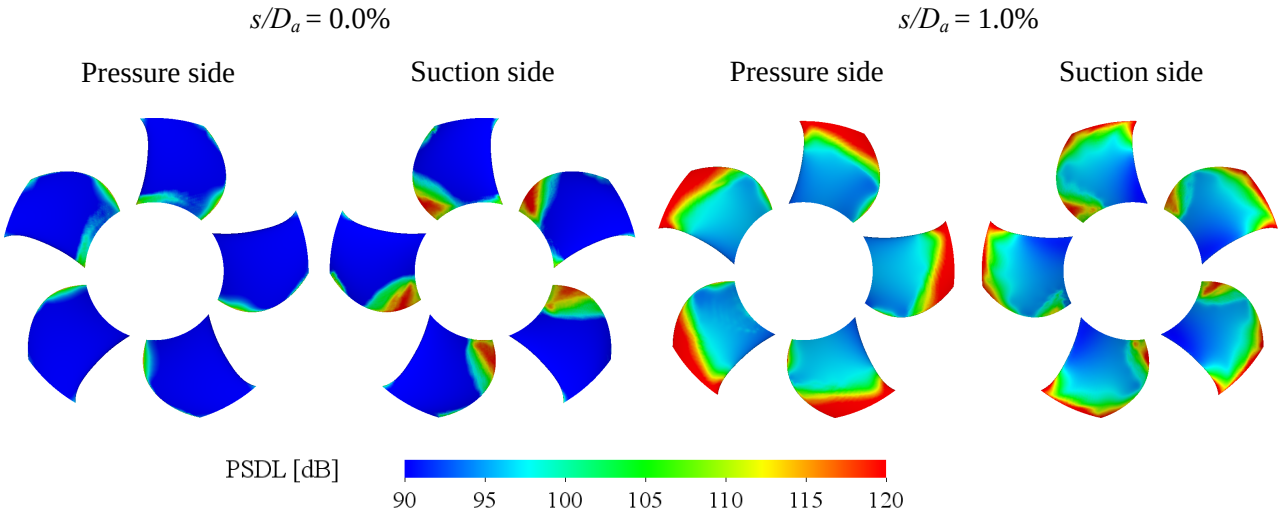

Figure 7. Power spectral density level of pressure fluctuations on the blade surfaces in a frequency band from 1 to 2 kHz.

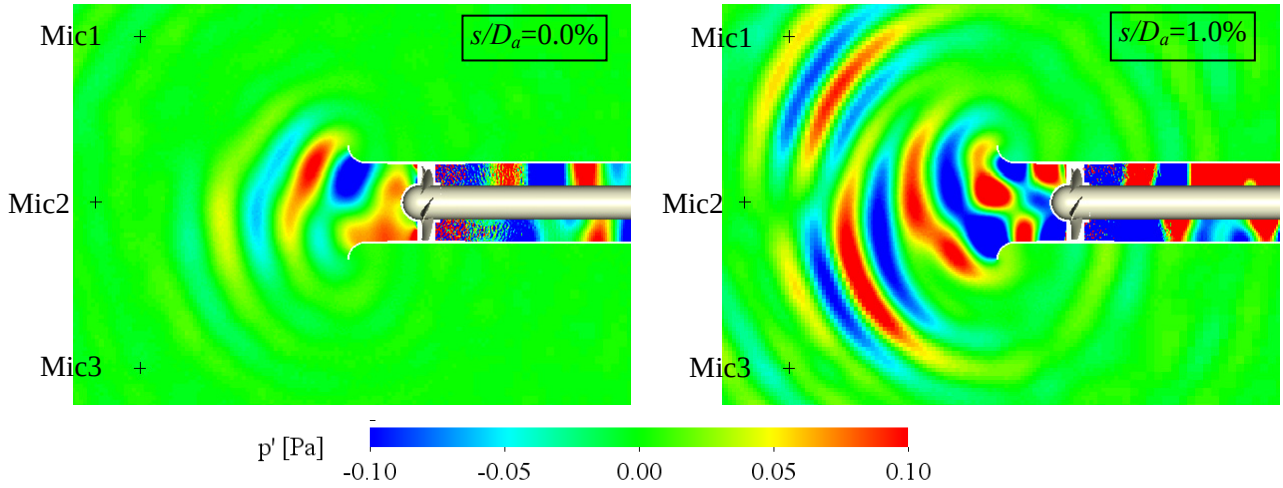

Figure 8. Instantaneous acoustic pressure radiated to the far field in the frequency band between 1 and 2 kHz

5. Conclusions

The LBM-predicted flow and acoustic field in the vicinity of an axial fan impeller's tip gap revealed important details of the sound generating mechanism. A large tip clearance is responsible for a complex vortex system with a considerable degree of inherent unsteadiness. The consequences are fluctuations of static pressure in the flow field in the adjacent tip region and on the blade surfaces, more pronounced on the pressure than on the suction side. Those pressure fluctuations generate sound that is then radiated away from the complete impeller upstream into the free field with the

typical hemispherical directivity pattern. Overall aerodynamic and acoustic fan performance data as predicted with the LBM were validated with experimental data. The agreement was quite satisfactory which justified looking at the LBM-predicted field data in detail. It would be of further value to validate "intermediate" quantities such as the surface pressure fluctuations on the stationary and rotating surfaces in the tip region, i.e. the acoustic sources themselves. Furthermore, varying the operation point of the fan and analyzing other ranges of frequencies where tonal components come into play, could be of great value for further understanding of tip clearance noise. It is expected that stall or so called rotating instabilities mix with the already complex tip flow. After all the sound directivity pattern in the free field upstream of the fan should be validated with appropriate experimental data.

6. Acknowledgements

The study was partly funded by the German Federal Ministry of Economics and Technology (BMWi) via the consortium for industrial research "Otto von Guericke" (AiF) and the Forschungsvereinigung Luft- und Trocknungstechnik e.V. (FLT).

REFERENCES

1. Longhouse, R. E., Control of Tip-Vortex Noise of Axial Flow Fans by Rotating Shrouds, *Journal of Sound and Vibration*, **58**, pp. 201-214, (1978).
2. You, D., Wang, M., Moin, P., and Mittal, R., Large-Eddy Simulation Analysis of Mechanisms for Viscous Losses in a Turbomachinery Tip-Clearance Flow, *Journal of Fluid Mechanics*, **586**, pp. 177-204, (2007).
3. You, D., Wang, M., Moin, P., and Mittal, R., Effects of Tip-Gap Size on the Tip-Leakage Flow in a Turbomachinery Cascade, *Physics of Fluids*, **18(10)**, pp. 105:102-114, (2006).
4. Fukano, T., and Jang, C.-M., Tip Clearance Noise of Axial Flow Fans Operating at Design and Off-Design Condition, *Journal of Sound and Vibration*, **275**, pp. 1027-1050, (2004).
5. Grilliat, J., Jacob, M. C., Camussi, R., and Caputi Gennaro, G., Tip Leakage Experiment - Part One: Aerodynamic And Acoustic Measurements, *Proc. 13th AIAA/CEAS Aeroacoustics Conference*, (2007).
6. Jacob, M. C., Grilliat, J., Camussi, R., Caputi Gennaro, G., Aeroacoustic Investigation of a Single Airfoil Tip Leakage Flow, *International Journal of Aeroacoustics*, **9(3)**, pp. 253-272, (2010).
7. Kameier, F., and Neise, W., Rotating Blade Flow Instability as a Source of Noise in Axial Turbomachines, *Journal of Sound and Vibration*, **203**, pp. 833-853, (1997).
8. März, J., Hah, C., and Neise, W., An Experimental and Numerical Investigation Into the Mechanisms of Rotating Instability, *Journal of Turbomachinery*, **124**, pp. 367-375, (2002).
9. Neuhaus, L., and Neise, W., Active Flow Control to Reduce the Tip Clearance Noise and Improve the Aerodynamic Performance of Axial Turbomachines, *Proc. Fan Noise 2003*, p. 8, (2003).
10. Corsini, A., Rispoli, F., and Sheard, A. G., Aerodynamic Performance of Blade Tip End-Plates Designed for Low-Noise Operation in Axial Flow Fans, *Journal of Fluids Engineering*, **131(8)**, pp. 081101:1-13, (2009).
11. Aktürk, A., and Camci, C., 2010, Axial Flow Fan Tip Leakage Flow Control Using Tip Platform, *Journal of Fluid Engineering*, **132**, (2010).
12. Aktürk, A., and Camci, C., Tip Clearance Investigation of a Ducted Fan Used in VTOL UAVS Part 2 Novel Treatments vis Computational Design and Their experimental Verification, *Proc. ASME Turbo Expo 2011*.
13. Zhu, T., and Carolus, T. H.., Experimental And Unsteady Numerical Investigation of the Tip Clearance Noise of an Axial Fan, *ASME 2013 Turbine Blade Tip Symposium & Course Week*, Hamburg, Germany, (2013).
14. Carolus, Th., Entwurfsprogramm für Niederdruckaxial-ventilatoren dAX-LP, 1987 - 2013.
15. U. Frisch, B. Hasslacher and Y. Pomeau, Lattice-Gas Automata for the Navier – Stokes Equations, *Phys. Rev. Lett.*, **56**, 1505-1508, (1986).
16. Guo, Z., Zhen, C. and Shi, B., Discrete Lattice Effects on the Forcing Term in the Lattice Boltzmann Method, *Phys. Rev. E.*, **65**, 046308, (2002).
17. Chen, H., Kandasamy, S., Orszag, S., Shock, R., Succi, S. and Yakhot, V., Extended Boltzmann Kinetic Equation for Turbulent Flows, *Science*, **301**, pp. 633-636, (2003).
18. Chen, H., Orszag, S., Staroselsky, I. and Succi, S., Expanded Analogy between Boltzmann Kinetic Theory of Fluid and Turbulence, *J. Fluid Mech.*, **519**, pp. 307-314, (2004).
19. Chen, H., Volumetric Formulation of the Lattice Boltzmann Method for Fluid Dynamics: Basic Concept, *Phys. Rev. E.*, **58**, pp. 2955-2953, (1998).
20. Kim, M.S., Pérot, F., Meskine, M., Aerodynamics and Acoustics Predictions of the 2-Blade NREL Wind Turbine using a Lattice Boltzmann Method, *14th International Symposium on Rotating Machinery,* (2012).
21. Pérot, F., Mann, A., Kim, M.S. and Fares, E., Advanced Noise Control Fan Direct Aeroacoustics Predictions using a Lattice-Boltzmann Method, *17th AIAA/CEAS Aeroacoustic Conference*, (2012).
22. Pérot, F., Kim, M.S., Le Goff, V., Carniel, X., Goth, Y. and Chassaignon, C., Numerical Optimization of the Tonal Noise of a Backward Centrifugal Fan using a Flow Obstruction, *Noise Control Engr. J.*, **61(3)**, (2013).
23. Zhang, R., Shan, X. and Chen, H., Efficient Kinetic Method for Fluid Simulation Beyond Navier-Stokes Equation, *Phys. Rev. E.*, **74**, 046703, (2006).
24. Sturm, M., and Carolus, T. H., Tonal Fan Noise of An Isolated Axial Fan Rotor Due to Inhomogeneous Coherent Structures at the Intake, *Noise Control Engineering Journal*, **60(6)**, pp. 699-706, (2012).